OPEN

Programmed death ligand-1 PET imaging in patients with melanoma: a pilot study

Neeta Pandit-Taskar[a,b], Audrey Mauguen[c], Denise Frosina[d], Achim Jungbluth[d], Klaus J. Busam[d], Serge Lyashchenko[a,b], Jazmin Schwartz[e], Parisa Momtaz[f,g], Allison Betof Warner[f,g], James W. Smithy[f], Alexander N. Shoushtari[f,g], Margaret K. Callahan[f,g], Paul B. Chapman[f,g] and Michael A. Postow[f,g]

Programmed death ligand-1 (PD-L1) is an inducible protein heterogeneously expressed in melanoma. Assessment of PD-L1 expression is challenging and standard immunohistochemistry (IHC) requires biopsies and cannot capture heterogeneity of expression. Noninvasive imaging methods provide evaluation of expression across lesions in the body. We conducted a prospective pilot trial with PD-L1 PET imaging with [^{18}F]-BMS-986229 as a noninvasive approach to assess PD-L1 expression across lesions, in 10 patients with advanced melanoma, longitudinally during treatment with nivolumab and ipilimumab. PET imaging was performed at baseline and at 6 weeks after initiation of treatment. We examined the relationship of PD-L1 PET uptake to radiographic clinical response. [^{18}F]-BMS-986229 uptake was variably seen across lesions in patients at baseline. All patients showed positive uptake in lesions at baseline PET with a median SUV_{max} of 3.6 (range: 1.7–8.6). PD-L1 PET SUV_{max} decreased in all but two lesions 6 weeks after treatment initiation. Four of five patients had a mean (SUV_{max}) greater than or equal to 3.00 in Response Evaluation Criteria in Solid Tumors (RECIST) evaluable lesions at baseline, and all had a RECIST response while all progressors ($n = 3$) had baseline PD-L1 mean SUV_{max} less than or equal to 2.60. A higher lesional baseline SUV_{max} was associated with greater individual lesion reduction during treatment. The PD-L1 uptake in lesions showed a low correlation with baseline PD-L1 by IHC. In this small pilot study, PD-L1 PET imaging using [^{18}F]-BMS-986229 showed feasibility in noninvasively assessing lesion uptake and PD-L1 heterogeneity in patients receiving combination immunotherapy. Future exploration of this tracer in larger patient cohorts is necessary to delineate its use in managing immunotherapy treatments. *Melanoma Res* 35: 328–338

Melanoma Research 2025, **35**:328–338

Keywords: [^{18}F]-BMS-986229, immunoPET, immunotherapy, melanoma, PD-L1

[a]Department of Radiology, Memorial Sloan Kettering Cancer Center, [b]Department of Radiology, Weill Cornell Medical College, Departments of [c]Epidemiology and Biostatistics, [d]Pathology, [e]Medical Physics and [f]Medicine, Memorial Sloan Kettering Cancer Center and [g]Department of Medicine, Weill Cornell Medical College, New York, New York, USA

Correspondence to Michael A. Postow, MD, Department of Medicine, Melanoma Service, Memorial Sloan Kettering Cancer Center, 1275 York Avenue, New York, NY 10065, USA
Tel: +1 646 888 4589; e-mail: Postowm@mskcc.org

Received 30 April 2025 **Accepted** 19 May 2025.

Introduction

Programmed cell death ligand-1 (PD-L1) is the most widely studied biomarker related to immunotherapy outcomes in melanoma and other cancers. Several immunotherapy treatments are approved only for patients whose tumors express PD-L1, including the nivolumab + relatlimab combination in Europe for patients with melanoma, making accurate assessment of PD-L1 critical for the appropriate use of immunotherapies [1]; however, evaluation of tissue expression of PD-L1 is not perfect in predicting immunotherapy responsiveness, potentially because of the fact that limited tissue sampling (such as with biopsies) cannot capture PD-L1 heterogeneity within large tumors or across different tumors within a patient [2,3]. Repeated biopsies to assess PD-L1 by immunohistochemistry (IHC) in this setting are logistically challenging and practically impossible for the assessment of individual lesions in all patients.

Whole-body PD-L1 PET imaging is an emerging strategy to comprehensively assess whole tumor burden PD-L1 expression over time. Prior imaging approaches have involved radiolabeling PD-L1 antibodies themselves such as ^{89}Zr-atezolizumab or ^{89}Zr-durvalumab [4,5] for assessment of expression of PD-L1 in tissues. These initial studies demonstrated the feasibility of imaging PD-L1 and showed heterogeneity across tumor types and variation in lesions in different sites. The heterogeneity

Supplemental Digital Content is available for this article. Direct URL citations appear in the printed text and are provided in the HTML and PDF versions of this article on the journal's website, www.melanomaresearch.com.

of target expression across patients and lesions was noted in bone versus soft tissue as well as across tumor types [4].

However, antibodies have longer clearance times and slower kinetics, often requiring several days to reach optimal target-to-background contrast in tissues. In a prior study using the ^{89}Zr-atezolizumab antibody, lesions were most optimally imaged at 4–7 days post-injection [4], adding the challenge of repeated patient visits and limiting ultimate clinical utility. In addition, the long half-life of the isotope used for radiolabeled antibodies combined with longer clearance times prevent early repeated imaging and restrict multiple longitudinal timepoint assessments of patients receiving treatment.

To circumvent the limitations of longer imaging times, lower molecular weight PD-L1 imaging agents such as the ~10 kDa fluorinated anti-PD-L1-radiolabeled adnectin [^{18}F]-BMS-986192 have been developed for PET imaging of tissue-specific binding to PD-L1 [6]. In initial clinical studies, [^{18}F]-BMS-986192 uptake has been shown to correlate with immunotherapy response and change in lesion size in small cohorts of patients [7,8]. Despite these favorable results, [^{18}F]-BMS-986192 was challenging to synthesize and is isolated only in modest radiochemical yields [6]. To facilitate broader clinical application of PD-L1 PET imaging, [^{18}F]-BMS-986229 was created as a macrocyclic peptide-based PET radioligand with similar properties to [^{18}F]-BMS-986192 (high affinity for PD-L1, tight binding with a slow off-rate from the receptor, rapid clearance from non-PD-L1-expressing tissues) but able to be isolated in higher yields [9]. BMS-986229 is a macrocyclic peptide (2 kDa) that targets PD-L1, and [^{18}F]-BMS-986229 is a PET tracer for whole-body assessment of PD-L1 expression.

Preclinical in-vitro and in-vivo evaluation of [^{18}F]-BMS-986229 demonstrates specific binding to PD-L1-expressing tissues [10]. In nonhuman primates, the uptake, rapid blood clearance, and short half-life with high target specificity lead to high contrast detection of tumors, enabling the feasibility of same-day imaging [10]. Projected data estimated from non-human primates, showed that the human absorbed dose in normal tissues, effective dose, and effective dose equivalent of [^{18}F]-BMS-986229 are comparable to other [^{18}F] tracers and similar imaging activity can be safely used as a PET radiotracer in humans. A recent study in 10 patients with esophageal, stomach, or gastroesophageal junction cancer, showed the safety and feasibility of whole-body PD-L1 assessment using [^{18}F]-BMS-986229 PET [11]. In that study, PD-L1 imaging was performed at only one baseline timepoint. Uptake of tracer was correlated with tissue evaluation that showed a strong correlation between the most avid lesion on PET, measured using standard uptake value (SUV) and uptake score, with PD-L1 combined positive score (CPS) [11].

To obtain a better understanding of how PD-L1 PET imaging with [^{18}F]-BMS-986229 changes in patients with melanoma during treatment with combination immunotherapy, we conducted a pilot study assessing PD-L1 PET in patients with advanced melanoma as the first examination of baseline and on-treatment PD-L1 PET imaging with [^{18}F]-BMS-986229. Melanoma is an ideal tumor type to explore PD-L1 imaging given heterogeneous responses to immunotherapy and the need to better define who truly needs combination immunotherapy given its higher toxicity burden.

Methods

This is a prospective pilot exploratory imaging study from a single institution as an additional cohort to a larger protocol, NCT03122522 (ClinicalTrials.gov ID). The protocol was approved by the institutional review board at Memorial Sloan Kettering Cancer Center (MSK), and all patients provided written informed consent.

Patients

Patients with unresectable stage III or IV melanoma who were treated with modified nivolumab 1 mg/kg and ipilimumab 3 mg/kg every 3 weeks as part of an additional expansion pilot cohort within the prospective Adaptively Dosed Immunotherapy Trial (ADAPT-IT; NCT03122522) were enrolled in this imaging study. Treatment with immunotherapy included two doses of nivolumab and ipilimumab, and if there were no new lesions nor an increase in index lesion tumor burden (>4%) at the time of first response assessment (week 6) using Response Evaluation Criteria in Solid Tumors (RECIST v1.1), patients stopped receiving the combination of nivolumab and ipilimumab and continued on nivolumab maintenance alone. If patients did not meet these prespecified protocol-defined metrics, they continued standard-of-care nivolumab and ipilimumab combination therapy for four doses before transitioning to nivolumab maintenance.

The aim of the pilot imaging study was to explore PD-L1 PET imaging, by assessing tracer uptake characteristics at baseline, before initiation of immunotherapy, and at follow-up on treatment at 6 weeks. The relationship of uptake at baseline and follow-up PD-L1 PET imaging was also examined in relation to the response measured by RECIST.

Radiolabeling of [^{18}F]-BMS-986229

PD-L1 PET imaging involved radiolabeling (BMT-180478) precursor obtained from Bristol Myers Squibb Inc. (Princeton, New Jersey, USA) under Investigational New Drug application #145622 by the radiochemistry and molecular imaging probes core facility at MSK using good manufacturing process methods. Following nucleophilic fluorination of the BMT-180478 precursor, a radiofluorinated intermediate was coupled to a peptide

precursor (BMT-196319) to generate the final imaging drug product [^{18}F]-BMS-986229 formulated in 10 ml of 10% ethanol in normal saline solution as previously described [9]. A dose of 370 MBq (10 mCi) ± 20% of [^{18}F]-BMS-986229 was administered intravenously over 1–2 min. No premedications were administered.

Imaging

Patients underwent PET imaging approximately 1 h after injection of the radiotracer based on prior imaging experience in patients (unpublished data; Bristol Myers Squibb Inc.) and as previously published [11].

PD-L1 PET images were acquired using a GE Discovery 710 PET/computed tomography (CT) scanner (GE Healthcare, Chicago, Illinois, USA). Each patient underwent whole-body PET/CT scans from the vertex of the skull to feet. Emission scans were acquired in three-dimensional mode at 3 min per field of view. PET/CT scans were performed with low-dose CT for attenuation correction. A single low-dose CT scan was obtained with 80 mA tube current (120 kVp; estimated radiation dose 9.0 mGy). Images were reconstructed with a 70 cm field of view into a 128 × 128 matrix using iterative ordered-subset expectation maximization (16 subsets; two iterations). All corrections recommended by the manufacturer were applied. Patients underwent second imaging on the same scanner and used the same parameters for injection and imaging as their first scan.

[^{18}F]-BMS-986229 PET/CT images were analyzed visually for tumor uptake. A site of abnormal increased uptake was defined as uptake clearly above normal adjacent background activity and not related to physiologic uptake. Lesion uptake was considered negative when visually clearly no uptake or less than background uptake. Uptake in sites of RECIST target and nontarget lesions was measured using maximum or mean SUV (SUV_{max} and SUV_{mean}, respectively). The lesion SUV was quantified by drawing volumes of interest (VOIs) on all positive sites using a 42% threshold [12]. VOIs were drawn on muscle (paraspinal) and aorta as an assessment of background activity. Uptake noted on baseline was re-evaluated at follow-up imaging at 6 weeks postinitiation of therapy. Uptake was measured using both maximum and average SUV (SUV_{max} and SUV_{mean}, respectively). All patients underwent diagnostic CT scans at baseline, 6, and 12 weeks per protocol and response was assessed in all patients based on CT RECIST 1.1 response criteria. Further follow-up was per clinical care and clinical outcome and response were assessed up to at least 3 months or earlier in the event of progression or death.

Pathologic correlation

Archival formalin-fixed, paraffin-embedded tissue was used for IHC analysis of PD-L1 with material available before protocol participation and the baseline PD-L1 PET scan. PD-L1 IHC was scored using the E1L3N antibody by tumor proportion score (TPS), immune cell score (ICS), and CPS as previously described [13].

Statistical analysis

In this exploratory analysis, data were summarized using frequencies (*N*) and percentages, and with median values and range. Analysis was performed at both the patient level and lesion level. For patient-level analyses, each patient's lesion uptake was summarized using the single highest lesion uptake per patient ($maxSUV_{max}$) and an average of all lesions' SUV_{max} ($meanSUV_{max}$). To explore the changes with treatment analysis was again performed at patient and lesion level. For patient-level analysis, change was examined in two ways. First, as the change in a single lesion with maximum ($maxSUV_{max}$), and second, as a change in the mean of all lesions' SUV_{max} (mean SUV_{max}), between the follow-up and baseline PD-L1 PET scans ($SUV_{follow\text{-}up} - SUV_{baseline}$).

Spearman coefficients were used to explore the correlation between the difference in individual target lesions' size on CT and differences in PD-L1 tracer uptake between imaging timepoints. For exploring the association between uptake signal and PD-L1 expression in tissue, the correlation between PD-L1 PET and IHC (TPS, ICS, and CPS) using SUV parameters from the biopsied lesion was estimated using Spearman's correlation coefficients. Progression-free survival (PFS) was defined as the time from the baseline PD-L1 PET scan to the progression of disease or death. Patients alive without progression were censored at the date of their last follow-up. PFS rates were estimated using the Kaplan–Meier estimator [14].

Results

Patients, PET scan completion, and programmed death ligand-1 PET safety

Ten patients underwent baseline PD-L1 PET imaging in the prospective pilot expansion cohort and received treatment with a modified combination of nivolumab and ipilimumab immunotherapy, as per a previously published protocol (Table 1) [15]. The median time from baseline PET scan to treatment start was 2 days; range of 1–7 days. Of the 10 patients who had baseline imaging, seven underwent follow-up on-treatment imaging (in week 6) following initiation of treatment. Three patients did not have follow-up on-treatment PD-L1 PET imaging because of either (a) early death from melanoma, (b) symptomatic progressive disease leading to inability to complete the PET, or (c) coronavirus disease–related logistical issues in a patient with partial response (PR). All patients tolerated the injection well, and there were no toxicities related to the [^{18}F]-BMS-986229 injection.

Table 1 Patient demographic

Characteristics	*N* = 10
Sex	
F	5 (50%)
M	5 (50%)
Age at treatment start	66 (50–84)
Stage	
IV A	1 (10%)
IV B	4 (40%)
IV C	4 (40%)
IV D	1 (10%)
Baseline LDH value	274 (156–2432)
Disease histology	
Cutaneous	9 (90%)
Unknown primary	1 (10%)
BRAF status (V600 mutant)	5 (50%)
Before any systemic therapy	1 (10%)
Before BRAF/MEK	
No	10 (100%)
Prior ipilimumab	
No	10 (100%)
Prior pembrolizumab or nivolumab	1 (10%)
Median (range), *n* (%)	

BRAF, serine/threonine-protein kinase B-Raf; F, female; LDH, lactate dehydrogenase; M, male; MEK, mitogen-activated protein kinase kinase.

Clinical outcomes

At week 6 postinitiation of treatment, out of the 10 patients, five had PR, two had stable disease, and three had progressive disease per RECIST [16] One of the patients with PR at 6 weeks evolved to a complete response at week 12, and one partial responder was not assessable at week 12, as they had withdrawn from the study. The remainder of the eight patients had no change in response from 6 to 12 weeks. The median PFS in this cohort was 11 months with an estimated 2-year PFS of 36% (95% confidence interval: 4–68%).

Tumor lesions available for clinical response and programmed death ligand-1 PET assessment

Among the 10 patients at baseline, 31 RECIST-measurable target lesions were identified on routine CT scans with respective organ sites of involvement as shown in Supplemental Table S1, Supplemental digital content, *https://links.lww.com/MR/A431*. The mean and median size of RECIST-measurable target lesions at baseline were 3.8 and 3.2 cm, respectively (range: 1.6–10.1 cm). Of the 31 RECIST target lesions noted on CT at baseline, 16 (52%) had detectable PD-L1 tracer uptake at baseline. The lesions that were positive on imaging primarily included nodes, soft tissue, adrenal, lung, and pleura (Supplemental Table S1, Supplemental digital content, *https://links.lww.com/MR/A431*). None of the liver lesions or peritoneal lesions noted on CT were positive on PD-L1 PET; liver lesions were photopenic compared with normal liver uptake.

Programmed death ligand-1 PET uptake in normal tissues and tumor lesions

PD-L1 PET distribution and [^{18}F]-BMS-986229 distribution showed physiological prominent uptake liver and spleen (Fig. 1) with low blood pool activity and mild diffuse uptake in other organs, similar to prior studies [8,11]. The blood pool activity at the time of imaging was low; uptake in the thoracic aorta ranged from 1.34 to 2.60 (median of 1.68). The tumor lesions were visually clearly delineated. There was no significant change in uptake SUV for liver, spleen, or blood pool in on-treatment imaging at 6 weeks.

Radiotracer uptake in tumor lesions was variable in baseline scans, with a median SUV_{max} of 3.6 (range: 1.7–8.6). At baseline, the meanSUV_{max} for all patients ranged from 1.9 to 8.6 and the maxSUV_{max} ranged from 1.9 to 8.6. When assessing changes in uptake from baseline to follow-up, PD-L1 SUV indices showed a trend toward slightly decreased uptake.

All patients with progressive disease at week 6 (n = 3) had maxSUV_{max} less than or equal to 2.6 (range: 1.9–2.6, median = 2.2) as compared to those with SD or PR (n = 7) who had maxSUV_{max} ranging from 2.1 to 8.6 (median = 5.2), and only one (i.e. 1/7) patient had maxSUV_{max} less than or equal to 2.6 (Fig. 2a). Similar results were observed for meanSUV_{max}, ranging from 1.9 to 2.6 (median = 2.2) in the patients with progressive disease, but ranged from 2.1 to 8.6 (median = 4) in patients with SD or PR, with only one patient having meanSUV_{max} less than or equal to 2.6 (Fig. 2b). For only patients with PR (n = 5), one had maxSUV_{max} of 2.1 while the other four had maxSUV_{max} ranging from 3.6 to 8.6; that is, four out of five had values higher than the ones observed in patients with progressive disease. The same results were observed for meanSUV_{max}: one patient had a value of 2.1 while the other four ranged from 3.6 to 8.6. Those values suggest that patients with PR or SD tend to have higher uptake than patients with progressive disease, although this is based on a small number of patients. Figures 1 and 3 show examples of high PD-L1 PET uptake in patients with favorable response to treatment whereas Fig. 4 shows negative PD-L1 PET uptake in a patient without response.

At week 12, four patients were still on treatment and considered responders by RECIST 1.1 (one CR and three PR). Three of these patients had baseline maxSUV_{max} greater than 2.6 (range: 3.6–5.4), while one patient had maxSUV_{max} of 2.1. Of note, SUV_{mean} was also investigated as a measure of uptake, but it did not show as much separation between responses (data not shown).

Programmed death ligand-1 PET and the response of individual tumor lesions

Given the intrapatient interlesional heterogeneity in lesion uptake and baseline PD-L1 SUV_{max} (Fig. 2e), we also sought to determine whether baseline PD-L1 tracer uptake within an individual lesion correlated with lesional response to combination immunotherapy. We evaluated all CT-identified RECIST target lesions

Fig. 1

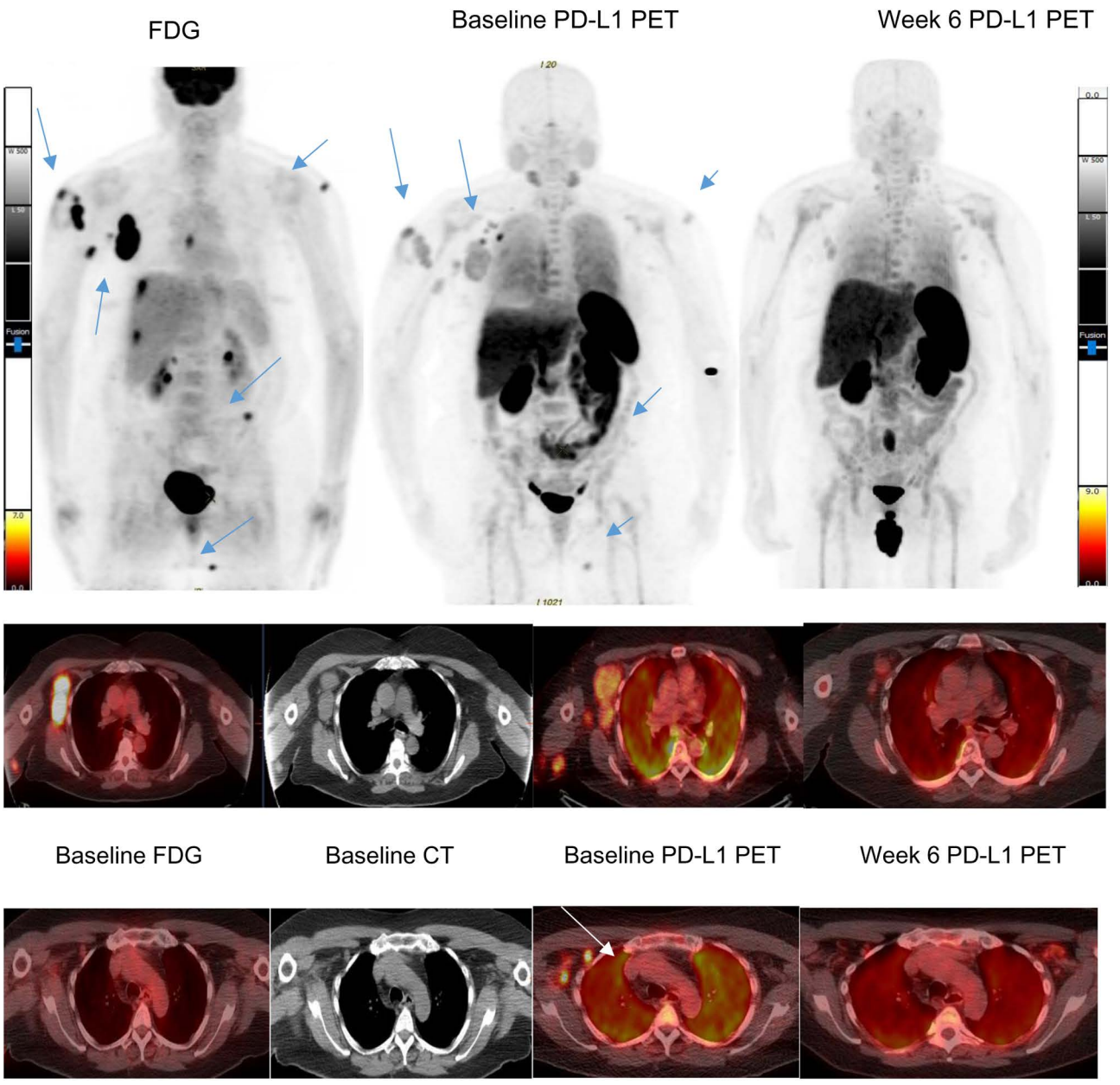

High PD-L1 PET uptake in responding patients. Patient with metastatic melanoma with soft tissue disease in the right arm, right axillary node, left shoulder cutaneous lesion, and left pelvic implants on baseline FDG PET (arrows) showing uptake on baseline PD-L1 PET imaging (arrows), which decreased on the week 6 PD-L1 PET. Some nodes in the subpectoral region (lower panel) show more prominent uptake on baseline PD-L1 PET than baseline FDG PET (white arrow). The patient had PR at 3 and 6 months follow-up. Diffuse uptake noted in the lung was not related to disease (not shown). Scale bars for FDG (left) and PD-L1 PET (right) are for all corresponding images. CT, computed tomography; FDG, fluorodeoxyglucose; PD-L1, programmed death ligand-1; PR, partial response.

for PET uptake at baseline and follow-up. For target lesions, the absolute change in size by RECIST 1.1 from baseline to week 6 (with negative numbers reflecting tumor reduction) was inversely correlated with baseline PD-L1 uptake ($r = -0.41$; Fig. 2c). In other words, a higher lesional baseline SUV_{max} was associated with greater lesion reduction in size on treatment. Changes in PD-L1 SUV from baseline to week 6 showed 10 of 12 lesions exhibiting a decrease (median: 2.2 decrease; range: 6.8 decrease–1.8 increase). A decrease in PD-L1 SUV_{max} between baseline and follow-up scan was moderately correlated with a decrease in lesional size by CT ($r = 0.35$; Fig. 2d). Heterogenous intrapatient uptake is shown in Fig. 5.

Fig. 2

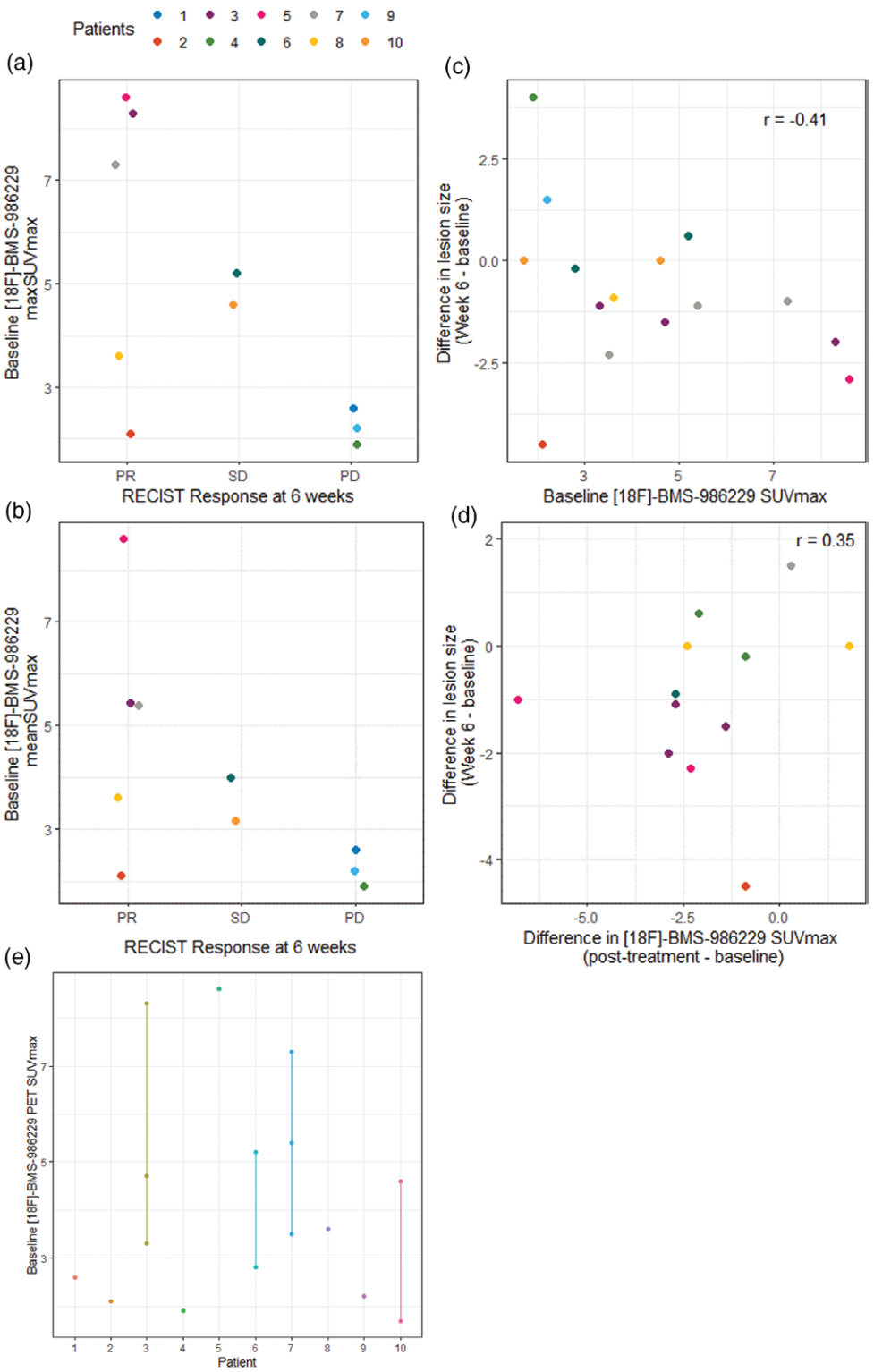

Patient- and lesion-based PD-L1 PET uptake and patient response. RECIST response per patient and baseline maxSUV_{max} of all measurable lesions within a patient (a) and meanSUV_{max} for all measurable lesions within a patient (b). Change in individual lesion size from baseline to week 6 by RECIST versus baseline individual lesion SUV_{max} (c) and change in PD-L1 PET individual lesion SUV_{max} from baseline to week 6 (d). Patients and lesions are missing from the plots because of missing follow-up CT scan (one patient and one lesion) and missing follow-up PD-L1 PET scan (three patientsand four lesions). Baseline target lesion PD-L1 PET uptake (e). Lines identify SUV_{max} range for patients with multiple lesions. CT, computed tomography; PD-L1, programmed death ligand-1; RECIST, Response Evaluation Criteria in Solid Tumors; SUV, standard uptake value.

Fig. 3

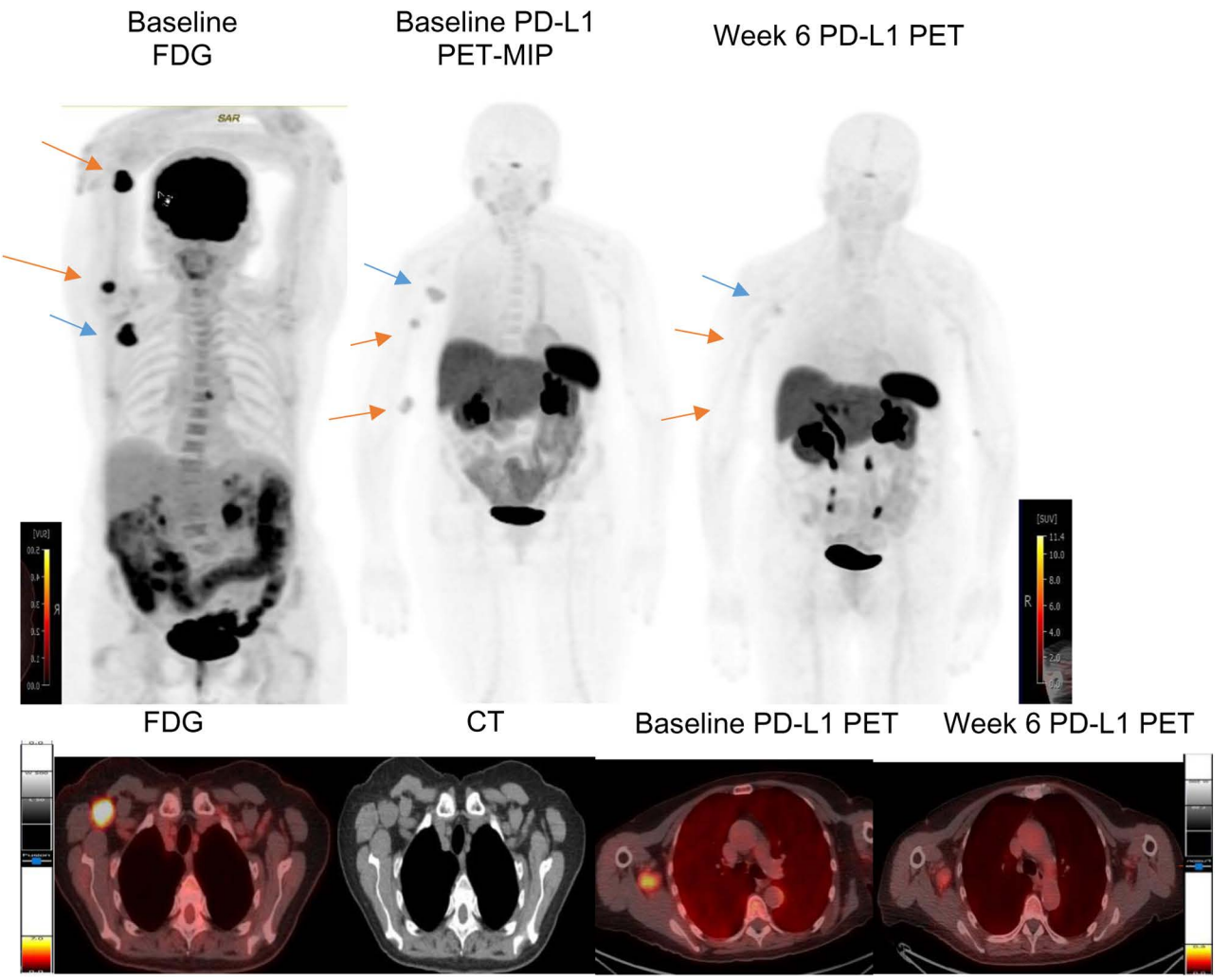

High PD-L1 PET uptake in responding patients. Patient with metastatic melanoma with soft tissue lesions in right arm (red arrows) and right axillary node (blue arrow) showing uptake on both baseline FDG and PD-L1 PET. This patient had decreased PD-L1 PET uptake in the right axillary node at week 6 and resolved uptake in the right arm lesions. The patient had PR at 3 and 6 months follow-up. Scale bars for FDG (left) and PD-L1 PET (right) are for all corresponding images. FDG, fluorodeoxyglucose; PD-L1, programmed death ligand-1; PR, partial response.

Among the 15 PD-L1 PET nonavid lesions, 12 were evaluable at 6-week follow-up CT. Six of the 12 lesions (50%) showed progression (range: +0.1 to +3.2 cm), and six lesions showed reduction (−0.1 to −5.6 cm) in size on CT scan. Three PD-L1-nonavid sites were not evaluable on follow-up (the patient died and did not have follow-up scans). None of the PD-L1-nonavid lesions on baseline scans showed any visual or quantifiable increased PD-L1 uptake of tracer in follow-up scans. Of the 16 PD-L1 PET-avid lesions at baseline, 15 were evaluable at 6 weeks: three (20%) progressed (+0.6 to +4.0), two were stable, and 10 (67%) had a reduction (−0.2 to −4.5). One of the PD-L1-avid sites was not evaluable on follow-up (the patient died and did not have follow-up scans).

Correlation between programmed death ligand-1 PET and programmed death ligand-1 immunohistochemistry

For nine patients where tissue was available for one lesion per patient, PD-L1 expression was assessed by standard IHC evaluating the PD-L1 TPS, ICS, and a CPS, with values ranging from 0 to 0.5 (Table 2). There was no clear separation of PD-L1 by IHC between overall patient immunotherapy response, among those patients assessable for RECIST responses (Supplemental Figure S1, Supplemental digital content, *https://links.lww.com/MR/A431*).

Correlation coefficients were close to zero between baseline PD-L1 PET SUV_{max} of the biopsied lesions and

Fig. 4

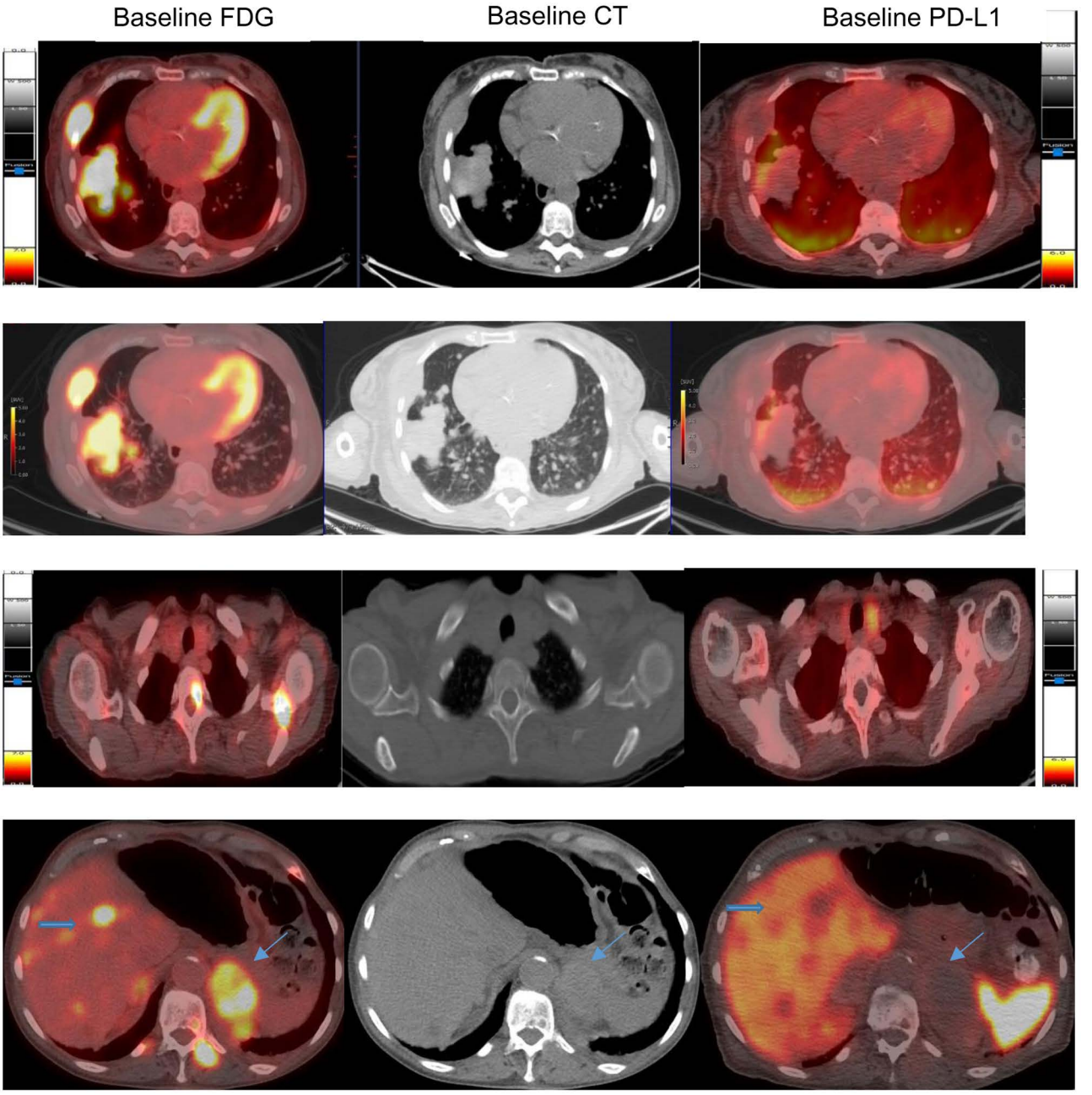

No PD-L1 PET uptake in nonresponding patients. Patient with metastatic melanoma with a right lung and a rib/intercostal muscle lesion seen on FDG PET (left top row) and CT scan (center top row). PD-L1 PET (right) imaging showed no uptake in the lung and rib/intercostal muscle lesions. Other FDG-avid lesions in bones (left middle row), liver (thicker arrow), and left adrenal (thin blue arrow, lowest row) also did not show uptake on PD-L1 PET. The patient had a progression of disease. Scale bars for FDG (left) and PD-L1 PET (right) are for all corresponding images. Lung uptake is noted in the posterior aspect; no corresponding CT abnormality was noted (second panel). CT, computed tomography; FDG, fluorodeoxyglucose; PD-L1, programmed death ligand-1.

PD-L1 IHC by TPS, ICS, and CPS ($r = 0.02$, 0.00, and 0.03, respectively); correlation coefficients were low to moderate between PD-L1 PET meanSUV_{max} (inclusive of all target lesions within a patient) and PD-L1 IHC ($r = 0.20$, 0.09, and 0.25, respectively).

Discussion

Imaging biomarkers that specifically target PD-L1 for assessing the presence and expression of the target using PET whole-body imaging allow for a more comprehensive assessment of the target across a patient's entire

Fig. 5

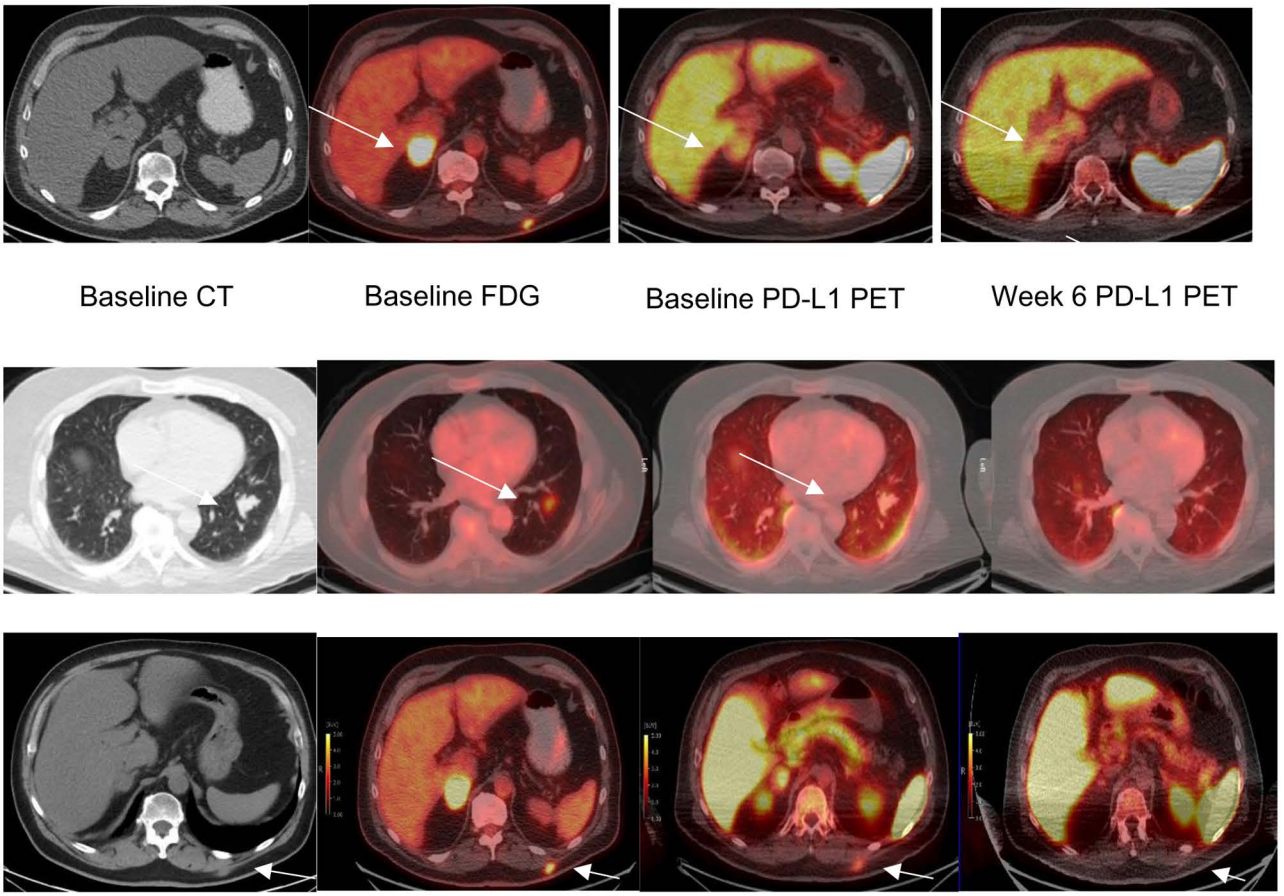

Heterogeneous baseline PD-L1 uptake among lesions. Patient with metastatic melanoma with left lung, right adrenal, and multiple soft tissue/subcutaneous nodules noted on FDG PET (arrows, fused images). On PD-L1 PET, these lesions showed heterogeneous uptake: the right adrenal lesion (4.3 cm) showing uptake on the baseline with decreased uptake in the follow-up scan (upper panel), lesion in the left lung (2.2 cm) (middle panel) showing no uptake, and left back subcutaneous nodule (1.6 cm) showing uptake (lower panel). The left back lesion showed resolution of uptake in follow-up imaging (right most fused image in the lower panel) and the right adrenal lesion shows decrease in uptake on follow-up PD-L1 imaging (the most right image in the top panel). This patient had PR radiographically at 3 and 6 months. FDG, fluorodeoxyglucose; PD-L1, programmed death ligand-1; PR, partial response.

metastatic melanoma burden. Serial imaging can thus provide critical information on the heterogeneity of target expression both at the initiation of treatment and at on-treatment timepoints to evaluate dynamic changes in PD-L1 expression during treatment. Distinct advantages of whole-body imaging over biopsies include avoiding invasive methods for tissue assessment and permitting multiple site assessments with one procedure. Several antibodies or smaller molecules have been radiolabeled and evaluated in early-phase clinical studies and have shown intra- and interpatient heterogeneity of target expression across lesions, but little remains known about how these PD-L1 PET agents perform in patients treated with combination immunotherapy, using both baseline and on-treatment imaging assessments [4,17].

Prior imaging with [^{18}F]-BMS-986192, a fluorinated anti-PD-L1 adnectin for PET imaging in patients with lung cancer has shown good targeting and uptake in tumor sites but significant heterogeneity between patients as well as within patients between different tumor lesions [8,17]. Similar heterogeneity of uptake was also noted in eight patients with metastatic melanoma [7]. In the only other study of [^{18}F]-BMS-986229, imaging was performed at only one baseline timepoint in patients with gastroesophageal tumors, 1 h postinjection, in accordance with past experience with a prior analog [8,11]. Our study expands on knowledge of PD-L1 PET imaging by exploring the feasibility of repeated imaging in patients undergoing combination immunotherapy, highly relevant for patients with melanoma given the frequent use of combination immunotherapy, and demonstrates the ability, for the first time, to dynamically evaluate changes in PD-L1 expression with treatment using [^{18}F]-BMS-986229.

Table 2 Programmed death ligand-1 immunohistochemistry results

Characteristic	*N* = 10
Tumor proportion score	
0	3 (33%)
0.02	2 (22%)
0.05	2 (22%)
0.1	2 (22%)
Unknown	1
Immune cell score	
0	2 (25%)
0.01	1 (12%)
0.1	1 (12%)
0.4	3 (38%)
0.5	1 (12%)
Unknown	2
Combined positive score	
0	3 (38%)
0.05	2 (25%)
0.12	1 (12%)
0.2	2 (25%)
Unknown	2

The biodistribution of [^{18}F]-BMS-986229 with the highest tracer uptake in the spleen, bone marrow, kidneys, and liver, is similar to prior observation with [^{18}F]-BMS986192 and expected given physiologic distribution of PD-L1 [7]. While data is limited, results showed that more lesions with PD-L1 PET SUV_{max} at baseline greater than 2.6, decreased in size on CT. This observation is similar to a prior study of [^{18}F]-BMS986192 in patients with metastatic melanoma that showed that baseline uptake predicted reduced lesion volume and was negatively correlated with the change in lesion diameter at the time of response evaluation [7]. Similar results were noted in the prior study with [^{18}F]-BMS-986229 in patients with gastroesophageal tumors, where patients who had [^{18}F]-BMS-986229 accumulation in any lesions on PET imaging had longer PFS following PD-1 based treatment than patients without tracer accumulation in any lesions [11]; however, in contrast to a prior study, we did not see any specific trend or increase in PD-L1 PET uptake on follow-up imaging compared with the baseline scan in patients with progressive disease [8]. It is likely that this may be because of the small number of patients and lesions and may also be because of the decreased size of lesions by the week 6 of treatment.

We found highly variable uptake in lesions, likely reflective of heterogenous PD-L1 expression across lesions and intrapatient heterogeneity (Fig. 5), which is similar to observations in prior studies with PD-L1 imaging [7,8,11]. Niemeijer *et al.* [8] noted marked intra- and interpatient heterogeneity of uptake and while a correlation of SUV_{peak} with response was seen, it was driven mainly by lesions with low uptake. In a subset of patients, the group noted a high uptake of tracer despite low expression. In similarity to their observation of higher SUV_{peak} of responding lesions versus nonresponding lesions, we noted a higher lesional baseline SUV_{max} associated with greater lesion reduction in size following treatment. In contrast, Nienhuis *et al.* [7] noted a negative correlation of [^{18}F]-BMS986192 uptake in lesions at baseline with the change in lesion diameter at response evaluation. In addition, though only in four patients with follow-up scans, the group noted that an increase in [^{18}F]-BMS986192 uptake from baseline scan correlated with an increased lesion size. We did not observe any significant relationship with the change in uptake, possibly because of small number of lesions.

Our study is limited because of small patient numbers; however, these preliminary results suggest the feasibility of using [^{18}F]-BMS-986229 imaging in assessing tumor PD-L1 expression and the potential relationship between baseline PD-L1 PET imaging lesion uptake and response to combination immunotherapy. We did not observe an obvious association between PD-L1 IHC and patient response, acknowledging limited data in our study, as tissue pathology via archival core biopsies was available only for a subset of patients and at varying timepoints before the baseline PD-L1 PET because of the infeasibility of obtaining fresh tumor biopsies before protocol participation for patients starting standard-of-care frontline immunotherapy for metastatic melanoma. Inherent PD-L1 heterogeneity within individual tumors and small tissue sampling are also likely contributing factors. It is likely that obtaining a PD-L1 PET-guided biopsy for IHC correlation may provide superior data for the correlation of imaging with IHC. In the future, a detailed assessment of uptake parameters is warranted, especially incorporating segmentation of uptake within lesion versus whole lesion uptake parameters.

Ultimately, if supported by larger studies, PD-L1 PET imaging could be helpful in patient management by better identifying patients whose tumors express PD-L1 and therefore may be the best candidates for immunotherapy, circumventing the known limitations of current patient selection based solely on PD-L1 IHC assessment using a single tumor biopsy. Moreover, longitudinal PD-L1 assessment during treatment may prove to be a useful tool in assessing the pharmacodynamic effects of investigational immunotherapies that act through CD8 cells and interferon-gamma signaling which is known to increase PD-L1 in the tumor microenvironment.

Conclusion

This exploratory prospective pilot study of patients with advanced melanoma provides the rationale for the exploration of PD-L1 PET imaging in larger cohorts to establish the potential of noninvasive, whole-body tumor burden immune profiling in patients undergoing immunotherapy. Additional research in larger cohorts is needed.

Acknowledgements

This work was supported in part by NIH/NCI Cancer Center Support Grant P30 CA008748. This research

was supported by Bristol Myers Squibb Inc, and the Radiochemistry & Molecular Imaging Probe Core of MSK, supported by NIH/NCI Cancer Center Support Grant P30 CA008748.

Conflicts of interest

M.A.P. reports consulting fees from BMS, Merck, Array BioPharma, Novartis, Incyte, NewLink Genetics, Aduro, and Eisai, and institutional support from RGenix, Infinity, BMS, Merck, Array BioPharma, Novartis, and AstraZeneca. N.P.-T. has served as a consultant or advisory board member for, and received honoraria from, Actinium Pharma, Progenics, MedImmune/AstraZeneca, Telix Pharma, Cellectar Illumina, and ImaginAb, and conducts research institutionally supported by Y-mAbs Therapeutics, ImaginAb, Telix, Cellectar, innervate, Fusion Pharma, BMS, Bayer, Clarity Pharma, Janssen, and Regeneron. For the remaining authors, there are no conflicts of interest.

References

1 Twomey JD, Zhang B. Cancer immunotherapy update: FDA-approved checkpoint inhibitors and companion diagnostics. *AAPS J* 2021; **23**:39.
2 Madore J, Vilain RE, Menzies AM, Kakavand H, Wilmott JS, Hyman J, *et al*. PD-L1 expression in melanoma shows marked heterogeneity within and between patients: implications for anti-PD-1/PD-L1 clinical trials. *Pigment Cell Melanoma Res* 2015; **28**:245–253.
3 McLaughlin J, Han G, Schalper KA, Carvajal-Hausdorf D, Pelekanou V, Rehman J, *et al*. Quantitative assessment of the heterogeneity of PD-L1 expression in non-small-cell lung cancer. *JAMA Oncol* 2016; **2**:46–54.
4 Bensch F, van der Veen EL, Lub-de Hooge MN, Jorritsma-Smit A, Boellaard R, Kok IC, *et al*. (89)Zr-atezolizumab imaging as a non-invasive approach to assess clinical response to PD-L1 blockade in cancer. *Nat Med* 2018; **24**:1852–1858.
5 Verhoeff S, van de Donk PP, Aarntzen E, Miedema IH, Oosting S, Voortman J, *et al*. 89Zr-durvalumab PD-L1 PET in recurrent or metastatic (R/M) squamous cell carcinoma of the head and neck. *J Clin Oncol* 2020; **38**:3573–3573.
6 Donnelly DJ, Smith RA, Morin P, Lipovšek D, Gokemeijer J, Cohen D, *et al*. Synthesis and biologic evaluation of a novel (18)F-labeled adnectin as a PET radioligand for imaging PD-L1 expression. *J Nucl Med* 2018; **59**:529–535.
7 Nienhuis PH, Antunes IF, Glaudemans A, *et al*. (18)F-BMS986192 PET imaging of PD-L1 in metastatic melanoma patients with brain metastases treated with immune checkpoint inhibitors: a pilot study. *J Nucl Med* 2022; **63**:899–905.
8 Niemeijer AN, Leung D, Huisman MC, Bahce I, Hoekstra OS, van Dongen GAMS, *et al*. Whole body PD-1 and PD-L1 positron emission tomography in patients with non-small-cell lung cancer. *Nat Commun* 2018; **9**:4664.
9 Donnelly DJ, Kim J, Tran T, Scola PM, Tenney D, Pena A, *et al*. The discovery and evaluation of [(18)F]BMS-986229, a novel macrocyclic peptide PET radioligand for the measurement of PD-L1 expression and in-vivo PD-L1 target engagement. *Eur J Nucl Med Mol Imaging* 2024; **51**:978–990.
10 Kim J, Donnelly DJ, Tran T, Pena A, Shorts AO, Petrone TV, *et al*. Development, characterization, and radiation dosimetry studies of (18) F-BMS-986229, a (18)F-labeled PD-L1 macrocyclic peptide PET tracer. *Mol Imaging Biol* 2024; **26**:301–309.
11 Cytryn SL, Pandit-Taskar N, Lumish MA, Maron SB, Gu P, Ku GY, *et al*. (18)F-BMS-986229 PET to assess programmed-death ligand 1 status in gastroesophageal cancer. *J Nucl Med* 2024; **65**:722–727.
12 Erdi YE, Mawlawi O, Larson SM, Imbriaco M, Yeung H, Finn R, Humm JL. Segmentation of lung lesion volume by adaptive positron emission tomography image thresholding. *Cancer* 1997; **80**:2505–2509.
13 Paver EC, Cooper WA, Colebatch AJ, Ferguson PM, Hill SK, Lum T, *et al*. Programmed death ligand-1 (PD-L1) as a predictive marker for immunotherapy in solid tumours: a guide to immunohistochemistry implementation and interpretation. *Pathology (Phila)* 2021; **53**:141–156.
14 Kaplan ELaM P. Nonparametric estimation from incomplete observations. *J Am Stat Assoc* 1958; **53**:457–481.
15 Postow MA, Goldman DA, Shoushtari AN, Betof Warner A, Callahan MK, Momtaz P, *et al*. Adaptive dosing of nivolumab + ipilimumab immunotherapy based upon early, interim radiographic assessment in advanced melanoma (the ADAPT-IT study). *J Clin Oncol* 2022; **40**:1059–1067.
16 Eisenhauer EA, Therasse P, Bogaerts J, Schwartz LH, Sargent D, Ford R, *et al*. New response evaluation criteria in solid tumours: revised RECIST guideline (version 1.1). *Eur J Cancer* 2009; **45**:228–247.
17 Huisman M, Niemeijer AL, Windhorst B, Schuit RC, Leung D, Hayes W, *et al*. Quantification of PD-L1 expression with [(18)F]BMS-986192 PET/CT in patients with advanced stage non-small-cell lung cancer. *J Nucl Med* 2020; **61**:1455–1460.